IAI Journals.ASM.org

Polymorphonuclear Leukocytes Restrict Growth of *Pseudomonas aeruginosa* in the Lungs of Cystic Fibrosis Patients

Kasper N. Kragh,[a] Morten Alhede,[a,b] Peter Ø. Jensen,[b] Claus Moser,[b] Thomas Scheike,[c] Carsten S. Jacobsen,[d] Steen Seier Poulsen,[f] Steffen Robert Eickhardt-Sørensen,[a] Hannah Trøstrup,[b] Lars Christoffersen,[b] Hans-Petter Hougen,[g] Lars F. Rickelt,[e] Michael Kühl,[e,h,i] Niels Høiby,[a,b] Thomas Bjarnsholt[a,b]

Department of International Health, Immunology and Microbiology, University of Copenhagen, Copenhagen, Denmark[a]; Department of Clinical Microbiology, Rigshospitalet, Copenhagen, Denmark[b]; Department of Public Health, Section of Biostatistics, University of Copenhagen, Copenhagen, Denmark[c]; Geological Survey of Denmark and Greenland, Copenhagen, Denmark[d]; Marine Biological Section, Department of Biology, University of Copenhagen, Helsingør, Denmark[e]; Department of Biomedical Science, University of Copenhagen, Copenhagen, Denmark[f]; Department of Forensic Medicine, University of Copenhagen, Copenhagen, Denmark[g]; Plant Functional Biology and Climate Change Cluster, University of Technology Sydney, New South Wales, Sydney, Australia[h]; Singapore Centre on Environmental Life Science Engineering, School of Biological Science, Nanyang Technological University, Singapore[i]

Cystic fibrosis (CF) patients have increased susceptibility to chronic lung infections by *Pseudomonas aeruginosa*, but the ecophysiology within the CF lung during infections is poorly understood. The aim of this study was to elucidate the *in vivo* growth physiology of *P. aeruginosa* within lungs of chronically infected CF patients. A novel, quantitative peptide nucleic acid (PNA) fluorescence *in situ* hybridization (PNA-FISH)-based method was used to estimate the *in vivo* growth rates of *P. aeruginosa* directly in lung tissue samples from CF patients and the growth rates of *P. aeruginosa* in infected lungs in a mouse model. The growth rate of *P. aeruginosa* within CF lungs did not correlate with the dimensions of bacterial aggregates but showed an inverse correlation to the concentration of polymorphonuclear leukocytes (PMNs) surrounding the bacteria. A growth-limiting effect on *P. aeruginosa* by PMNs was also observed *in vitro*, where this limitation was alleviated in the presence of the alternative electron acceptor nitrate. The finding that *P. aeruginosa* growth patterns correlate with the number of surrounding PMNs points to a bacteriostatic effect by PMNs via their strong O_2 consumption, which slows the growth of *P. aeruginosa* in infected CF lungs. In support of this, the growth of *P. aeruginosa* was significantly higher in the respiratory airways than in the conducting airways of mice. These results indicate a complex host-pathogen interaction in chronic *P. aeruginosa* infection of the CF lung whereby PMNs slow the growth of the bacteria and render them less susceptible to antibiotic treatment while enabling them to persist by anaerobic respiration.

Patients with the genetic disorder cystic fibrosis (CF) have highly viscous endobronchial mucus and decreased mucociliary clearance of the airways, which render them susceptible to chronic bacterial lung infections. Severe chronic *Pseudomonas aeruginosa* lung infections are the most common cause of morbidity and mortality in CF patients (1, 2). Lungs of CF patients with chronic *P. aeruginosa* infections are characterized by intrabronchial mucus-imbedded aggregates of bacterial cells (biofilms) surrounded by high numbers of polymorphonuclear leukocytes (PMNs) (3, 4). Such PMN-surrounded biofilms can persist over the lifetime of CF patients, despite an extensive inflammatory response and aggressive antibiotic treatment (5).

Slow growth within bacterial biofilms is recognized as a major contributor to high antibiotic tolerance because the effectiveness of the majority of antibiotics in clinical use decreases with low bacterial metabolism (6, 7). Limited molecular oxygen (O_2) can further increase the tolerance of *P. aeruginosa* biofilms for antibiotics *in vitro* (8). Mucus in the conducting airways of chronically infected CF patients is characterized by steep O_2 concentration gradients ranging from normoxic to anoxic conditions, and the combination of slow diffusive transport and intense O_2 consumption within the mucus leads to anoxia (9). This is accompanied by ongoing denitrification, as evidenced by N_2O production (10), the denitrification biomarker OprF in sputum (11), antibodies against nitrate reductase in serum (12), and upregulation of genes for denitrification (13, 14). O_2 gradients in the endobronchial secretions are primarily a result of the O_2 consumed by PMNs for the formation of reactive oxygen species (15, 16) during respiratory burst (15, 16) and for the production of nitric oxide (10) by nitric oxide synthase (54, 55). In addition, the fraction of O_2 consumed by PMNs for aerobic respiration in endobronchial secretions from chronically infected CF patients is negligible (15, 16). The growth rate of *P. aeruginosa* is diminished by the low availability of O_2 (17); therefore, depletion of O_2 within the mucus of CF patients could serve as a limiting factor for the growth of *P. aeruginosa* and may contribute to the slow growth of *P. aeruginosa* in the sputum of chronically infected CF patients (18). Alternatively, it has been suggested that isolates from chronically infected CF patients may develop genetic adaptations that reduce the growth rate of the bacteria (19). Under these conditions, the above-mentioned denitrification indicators point to anaerobic respiration using nitrate as an alternative metabolic mode of *P.*

Received 24 April 2014 Returned for modification 11 July 2014
Accepted 5 August 2014
Published ahead of print 11 August 2014
Editor: B. A. McCormick
Address correspondence to Thomas Bjarnsholt, tbjarnsholt@sund.ku.dk.
Supplemental material for this article may be found at http://dx.doi.org/10.1128/IAI.01969-14.

doi:10.1128/IAI.01969-14

aeruginosa, resulting in lower energy yields and possibly lower growth rates in biofilms in the CF lung. However, only the *in vitro* growth of bacteria isolated from sputum samples has been studied (18), and the actual growth rates of *P. aeruginosa* within CF lungs have neither been mapped nor correlated to growth limitation *in vivo*.

In this study, we developed a new quantitative peptide nucleic acid fluorescence *in situ* hybridization (PNA-FISH)-based method that enabled mapping of the *in vivo* growth rates of *P. aeruginosa* for the first time. This method was used to investigate the growth of *P. aeruginosa* in chronically infected CF lungs and in the conducting and respiratory airways of *P. aeruginosa*-infected mice. A significant negative correlation was observed between the growth rate and the abundance of PMNs surrounding the bacterial biofilm aggregates. A strong PMN-induced O_2 limitation on *P. aeruginosa* growth was confirmed *in vitro*, while the bacterial growth limitation was alleviated in the presence of an alternative electron acceptor (nitrate) that enabled denitrification.

MATERIALS AND METHODS

Bacterial strains. The *P. aeruginosa* PAO1 wild-type strain used in all *in vitro* experiments was obtained from the *Pseudomonas* Genetic Stock Center (strain PAO0001 [http://www.pseudomonas.med.ecu.edu]). The *Escherichia coli* laboratory strain MG1655 was used for production of spike-in DNA (20).

***Ex vivo* CF patient samples.** Samples were obtained from explanted lungs of three CF patients chronically infected with *P. aeruginosa* (one male and two females ranging from 30 to 42 years old). Tissue was collected following approval (KF-01278432) from the Danish Scientific Ethical Board. All three patients had undergone double-sided lung transplantation at the Copenhagen University Hospital, Rigshospitalet. Lung tissue samples ($n = 6$ to 7 from each patient) were removed immediately after extraction. Samples ($n = 20$) were fixed in phosphate-buffered saline containing 4% paraformaldehyde and embedded in paraffin. Sections (4 μm thick) were cut using a standard microtome and fixed on glass slides. The slides were stored at 4°C until further analysis. In total, 59 bacterial biofilms were analyzed.

Mouse model. To examine differences in bacterial growth rate as a function of O_2 partial pressure, we used a recently described model based on the instillation of bacteria immobilized on small or large alginate beads into the respiratory or conducting zone of the lungs (21). Briefly, the *P. aeruginosa* strain PAO579 was propagated overnight at 37°C in ox broth (Statens Serum Institute, Denmark). The overnight culture was centrifuged at 4°C and 4,400 × *g* and resuspended in 5 ml of serum bouillon (Department of Clinical Microbiology, Herlev Hospital, Denmark). Alginate (Protanal LF 10/60; FMC BioPolymer, Norway) was dissolved in 0.9% NaCl to a concentration of 1% and sterile filtered. The bacterial culture was diluted 1:20 in the alginate solution. The solution was transferred to a 10-ml syringe and placed in a syringe pump (model 3100; Graseby, United Kingdom), which fed the alginate to the encapsulation unit (Var J30; Nisco Engineering, Zurich, Switzerland). The alginate was pumped into a gelling solution of 0.1 M $CaCl_2$ prepared in 0.1 M Tris-HCl buffer (pH 7.0), which was agitated with a magnetic stirrer (RCT Basic; IKA, Germany). The beads stabilized under continuous stirring in the gelling bath for 1 h and were then washed twice with 0.9% NaCl containing 0.1 M $CaCl_2$ before being transferred to 20 ml of 0.9% NaCl containing 0.1 M $CaCl_2$. Five milliliters of alginate beads was prepared, with mean bead diameters of 136 μm (range, 74 to 205 μm; $n = 72$) and 40 μm (range, 15 to 85 μm; $n = 72$) for large and small beads, respectively.

The number of bacteria in the alginate beads was determined by dissolving the beads in 0.1 M citric acid buffer (pH 5.0) and plating the supernatant for CFU counts.

BALB/c female mice (11 weeks old; Taconic Europe A/S, Denmark) were allowed to acclimatize for 1 week before use. The mice had free access to chow and water and were handled by trained personnel. All animal experiments were authorized by the National Animal Ethics Committee, Denmark.

Mice were anesthetized subcutaneously with a 1:1 mixture of etomidate (Janssen, Denmark) and midazolam (Roche, Switzerland) (10 ml/kg body weight) and then tracheotomized. Alginate beads embedded with *P. aeruginosa* PAO579 were installed in the left lung of BALB/c mice using a bead-tipped needle. All mice received similar amounts of alginate beads and *P. aeruginosa* cells (1×10^8 CFU/ml for both groups).

Eight mice (four with each size of aggregate beads) were examined each day; two mice from both groups were euthanized at 0, 1, 3, and 5 days after bacterial inoculation. The left lungs were fixed in a 4% (wt/vol) formaldehyde solution (VWR, Denmark). Bacterial growth was measured in 34 aggregates (14 aggregates from respiratory airways and 20 aggregates from conducting airways).

Quantitative PNA-FISH. Paraffin-embedded samples were deparaffinized by treatment with xylene (twice for 5 min), 99.9% ethanol (EtOH; twice for 3 min), and 96% EtOH (twice for 3 min) and were then washed in MilliQ water three times for 3 min. A drop of a Texas Red-conjugated PNA-FISH probe specific for *P. aeruginosa* 16S rRNA (AdvanDx, USA) was applied to the tissue section and then covered with a coverslip (22). Samples were incubated for 90 min at 55°C (AdvanDx Workstation, AdvanDx, USA). The coverslip was removed, and the slides were washed in warm washing buffer at 55°C (AdvanDx, USA) for 30 min and then air dried in the dark. A drop of Vectashield mounting medium with 4′,6′-diamidino-2-phenylindole (DAPI; Vector, USA) was placed on top of the slide, which was then covered with a coverslip (Menzel-Glaser, Germany) and air dried for 15 min.

Mounted slides were scanned using a confocal laser scanning microscope (CLSM) (Axio Imager.Z2, LSM710 CLSM; Zeiss) and the accompanying software (Zen 2010, version 6.0; Zeiss, Germany). Extremely high resolution and color depth are required for precise quantification. Therefore, fluorescence images were recorded at an emission wavelength of 615 nm with a resolution of 6,144 by 6,144 pixels and at a color depth of 16 bits with a 63×/1.4 (numerical aperture) oil objective using laser excitation at 594 nm. Each pixel was scanned twice. Images were stored in 16-bit TIF format. Fluorescence in individual cells was quantified using the freeware program ImageJ (National Institutes of Health, Bethesda, MD, USA). The background signal was defined by a threshold value using the automated MultiThresholder macro for ImageJ (K. Baler, G. Landini, and W. Rasband, NIH, Bethesda, MD). For quantification, the ImageJ function "analyze particles" was used. The fluorescence intensity was calculated in fluorescence units (FU) as the mean of gray-scale units over a range from 0 to 65,535. The correlation between FU and growth rate was used to estimate the growth rate (see Fig. 2; see also Supplemental Materials and Methods in the supplemental material). Using a correlation can result in the prediction of a negative growth rate. Growth rates cannot be less than zero; therefore, in these cases, the growth rate was considered to be slow.

The length, width, and cross-sectional area of biofilm aggregates in lung tissue samples from CF patients, as well as the distances from individual biofilms to the edge of their mucus clumps in the lung tissue, were measured using Zeiss Zen 2010, version 6.0. A proxy for the level of inflammation and PMN activity around each biofilm aggregate was obtained by counting all PMNs stained with DAPI within a distance of 20 μm from the edge of the biofilm using Zeiss Zen 2010, version 6.0.

PMNs on *P. aeruginosa in vitro*. One hundred milliliters of Krebs-Ringer buffer (KRB) (Panum Institute, Denmark) supplemented with 1% glucose was inoculated with 100 μl of PAO1 and incubated overnight at 37°C in a shaker. When the culture reached an optical density at 450 nm (OD_{450}) of 0.2, it was diluted to an OD_{450} of 0.1 using KRB containing glucose at 37°C, after which 500 μl was added to the airtight lower chamber of a 0.2-μm single-step filter vial (Thomson, USA) (see Fig. 7). Human blood was collected from healthy volunteers with the approval (H-3-2011-117) of the Danish Scientific Ethical Board. PMNs were isolated as described elsewhere (23). Extracted PMNs were resuspended in KRB con-

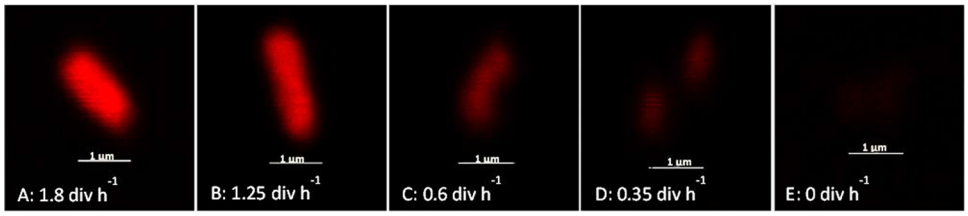

FIG 1 *Pseudomonas aeruginosa* at different growth rates. The cells were treated with PNA-FISH probes targeting *P. aeruginosa* 16S rRNA. The specific growth rates, in divisions (div) per hour, are indicated on the panels.

taining glucose at 37°C to a final density of 2.5×10^7 PMNs/ml. In total, 200 μl of the PMN suspension was added to the chamber above the filter, while the chamber below the filter received 200 μl of KRB containing glucose. Half of both the PMN-treated and untreated vials was supplemented with 10 mM KNO_3, and the vials were incubated at 37°C. After 0, 2, and 4 h, 20 μl of bacterial suspension from the airtight chamber was fixed on Super Frost Plus slides (Thermo Scientific, USA) with GN Fixation Solution (AdvanDx, USA) at 65°C for 20 min. Slides were analyzed by quantitative PNA-FISH as described above.

O_2 levels in the lower, airtight chamber containing the bacteria and in the upper chamber containing the PMNs were measured using O_2-sensitive sensor spots mounted inside the vials and monitored with a fiber-optic O_2 meter (Fibox 3; PreSens, Germany) equipped with a 2-mm fiber-optic cable (24, 25). PMN activation was induced by 10 μM phorbol 12-myristate 13-acetate (PMA) (Sigma-Aldrich, USA).

Statistical analysis. Statistical significance was evaluated using a Mann-Whitney test. Multiple regressions were used to evaluate multifactor models of data. To evaluate relationships without parametric assumptions, Spearman's rank correlation was used. *P* values of <0.05 were considered to be significant. All tests were performed using GraphPad Prism, version 5 (GraphPad Software, USA) and InStat, version 3 (GraphPad Software).

RESULTS

Schaechter et al. defined a proportional relationship between the rate of growth and the ribosomal content in *Salmonella enterica* serovar Typhimurium cells (26), enabling estimates of the bacterial growth rate from the number of ribosomes. Fluorescently conjugated PNA was hybridized to the RNA of intact ribosomes in *P. aeruginosa* cells, and the fluorescent signal was correlated to the growth rate of the bacteria. Based on the use of quantitative PNA-FISH and real-time PCR (RT-PCR) specific for *P. aeruginosa* 16S rRNA, the ribosomal content of *in vitro* pure culture samples taken at different growth phases was determined. The specific growth rate was calculated at the exact sampling time based on optical density (OD) measurements. For each sample, the average number of fluorescence intensity units (FU) emitted by the PNA-FISH-treated cells was quantified. Between 10 and 200 cells were measured at each time point, and the number of rRNA molecules per rRNA gene molecule (i.e., the number of ribosomes per ribosome/protein-encoding gene, or the number of ribosomes) was quantified by RT-PCR. Fluorescence microscopy showed a clear difference in the fluorescence intensity of cells sampled at different growth rates (Fig. 1).

Correlating fluorescence to growth rate. The mean number of FU emitted in pixels, within a threshold that discriminates background fluorescence, was plotted as a function of the number of ribosomes in each sample. Samples were taken to represent cultures in exponential growth, decreasing growth, and stationary phase (labeled green, yellow, and red, respectively, in Fig. 2).

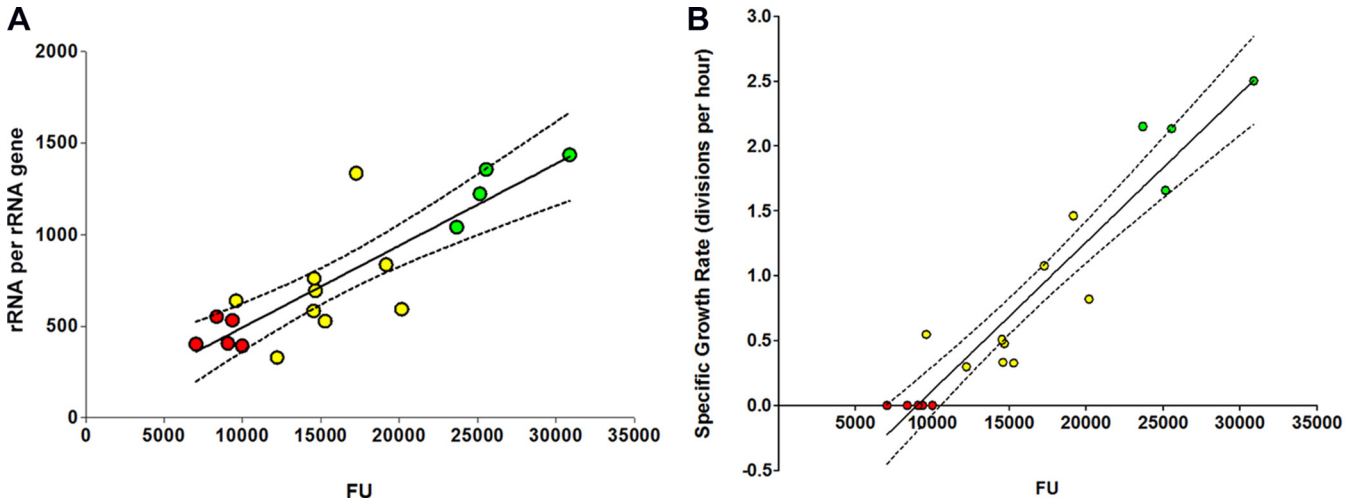

FIG 2 Correlations between fluorescence intensity and rRNA or growth rate. (A) Correlation between the average fluorescence intensity in *P. aeruginosa* cells and the number of rRNA molecules per rRNA gene molecule, as measured by RT-PCR. The black line shows the calculated correlation, and the two dotted lines show the 95% confidence interval. The correlation has an R^2 fit at 0.7222. The relationship is described by $y = 0.0447 \times x + 46.3$. (B) Correlation between the average measured fluorescence intensity (FU) in *P. aeruginosa* and the growth rate determined from OD measurements of bacterial culture samples as a function of time. The black line shows the calculated correlation, and the two dotted lines show the 95% confidence interval. The correlation has an R^2 fit at 0.7627. The relationship is described by $y = (1.146 \times 10^{-4}) \times x - 1.031$.

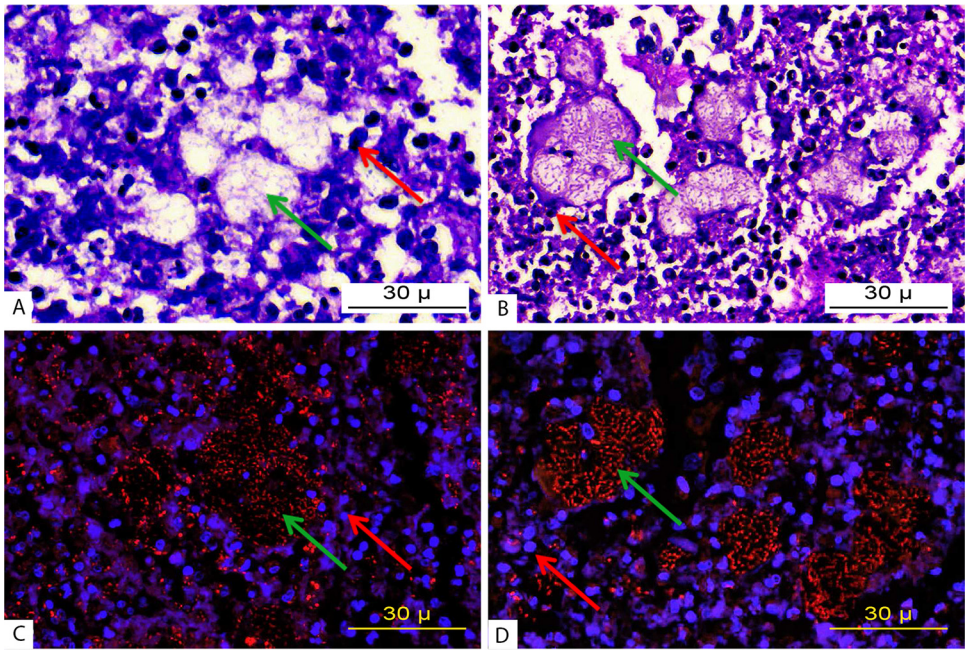

FIG 3 Micrograph of *P. aeruginosa*-infected lung tissue. Light and fluorescence microscopy images (magnification, ×170) of periodic acid-Schiff- and hematoxylin-stained sections (A and B) and PNA-FISH-stained sections (C and D) containing luminal and mucosal accumulations of inflammatory cells. The *P. aeruginosa*-positive areas are seen as well-defined lobulated clarifications surrounded by inflammatory cells. Red arrows indicate PMNs, and green arrows indicate *P. aeruginosa* biofilm aggregates.

There was a significant ($P < 0.0001$) linear correlation between FU values and rRNA: number of rRNA molecules per rRNA gene molecule = $0.0447 \times \text{FU} + 46.3$ ($R^2 = 0.722$) (Fig. 2A). The lack of a linear relationship and normally distributed residuals for low levels of FU does not invalidate our conclusion of a significantly positive relationship, as shown by the computed Spearman's correlation ($\rho = 0.7936$, $P < 0.0001$). As the specific growth rates were known for each sample, the fluorescence intensity and the rRNA content could be expressed as a function of the growth rate and *vice versa*. There was also a significant ($P < 0.0001$) linear correlation between FU and the specific growth rate: growth rate = $(1.146 \times 10^{-4}) \times \text{FU} - 1.031$ ($R^2 = 0.763$) (Fig. 2B). These relationships enabled us to estimate the growth rate based on fluorescence intensity measurements. The few outliers that prevent a normal distribution of the data did not alter the statistically significant positive relationship (Spearman's correlation, $\rho = 0.9104$; $P < 0.0001$).

Environmental regulation of ribosomal activity. Quantitative PNA-FISH was used in two starvation experiments to investigate ribosomal content in *P. aeruginosa* in response to sudden carbon/nitrate starvation and O_2 depletion. When the exponentially growing culture was deprived of all carbon or nitrogen sources, a decline in the FU value was observed that could be described as a mono-exponential decay (see Fig. S1A in the supplemental material) ($R^2 = 0.93$), with an FU decay constant of 58.9% h^{-1}, which reached an asymptotic value of 8,558 FU after 6 to 7 h. This correlated well with findings from the growth phase study showing a baseline of 8,800 ± 932 FU (mean ± standard deviation [SD]) in cells from a very late stationary phase (≥24 h after inoculation). When cells were exposed to a sudden shift from oxic to anoxic conditions, resulting in O_2 depletion, a similar exponential decay of FU ($R^2 = 0.91$ and FU decay constant of 51.4% h^{-1}) was observed, which reached an asymptotic level of 8,267 FU after 7 h of anoxia (see Fig. S1B).

Growth rates in clinical samples. To directly estimate the growth of *P. aeruginosa* in the lungs of end-stage CF patients, the quantitative PNA-FISH method was used on explanted lungs from three CF patients. Tissue samples ($n = 20$) were collected to represent all regions of the infected lungs. Many biofilm aggregates were embedded in mucus in the conducting zone and were surrounded by PMNs, consistent with earlier observations (4) (Fig. 3). Using quantitative PNA-FISH, the mean specific growth rate was estimated in each of the biofilm aggregates ($n = 59$). A high variability in growth rate was found among the samples from all three patients, ranging from 0 to 0.90 divisions per hour (Fig. 4). Similar heterogeneity was also observed within each tissue section. In a 1-cm^2 section, growth rates ranging from 0 to 0.65 divisions per hour were observed. Interestingly, bacteria isolated just prior to lung transplantation were not growth limited *in vitro* as the median growth rate was estimated to be 1.2 divisions per hour (range, 1.15 to 1.60), which is significantly ($P \leq 0.0058$) higher than the *in situ* growth rate of 0.217 divisions per hour (range, −0.10 to 0.67).

Effects of biofilm aggregate size, depth, and diameter on growth rate. The size, depth within the mucus, and diameter of each biofilm aggregate in the CF lung samples were measured, and possible synergistic correlations to the *in vivo* growth rates of *P. aeruginosa* were investigated by multiple regression analysis. No significant synergistic interactions were found that could explain the observed heterogeneity of the bacterial growths rates, such as size, depth, and diameter ($P \leq 0.3665$), size and depth ($P \leq 0.2413$), size and diameter ($P \leq 0.4513$), or depth and diameter ($P \leq 0.6841$). The average size of the biofilm aggregates was 520

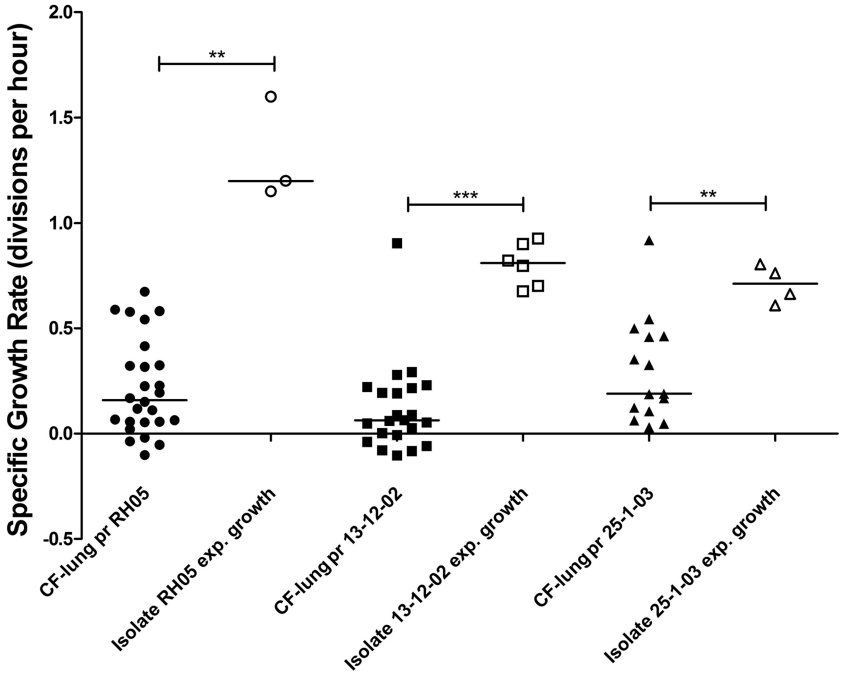

FIG 4 Growth rates measured in lung tissue and peak growth rate achieved by isolates. The specific growth rate of *Pseudomonas aeruginosa* was estimated by quantitative PNA-FISH in 59 biofilm aggregates in 20 tissue sections from explanted lungs from three CF patients (solid symbols). The highest exponential (exp) growth measurements from isolates are shown as open symbols. The horizontal line represents the median rate in each patient. Dates of sampling are indicated. pr, patient; **, $P \leq 0.01$; ***, $P \leq 0.001$.

μm^2 (range, 4 to 3,227 μm^2). The lack of correlation between growth rate and size is depicted in Fig. 5.

PMN counts and effects on *P. aeruginosa* growth. While aggregate size and location do not affect growth rate in the CF lung, an alternative explanation is that slower-growing aggregates may be limited for an important nutrient. Previous observations show that PMNs increase their O_2 consumption upon contact with bacteria *in vitro* (11, 27); we hypothesized that slow-growing aggregates may be surrounded by significantly higher levels of PMNs than aggregates with a higher growth rate. The number of PMNs was counted within 20 μm around each biofilm aggregate, and a significant inverse correlation was found ($\rho = -0.4471$, $P < 0.0004$) between the PMN count and the *in vivo* growth rate of *P. aeruginosa* (Fig. 6).

***In vitro* confirmation of a biostatic function of PMNs.** To test whether PMNs can limit the growth of *P. aeruginosa*, bacterial

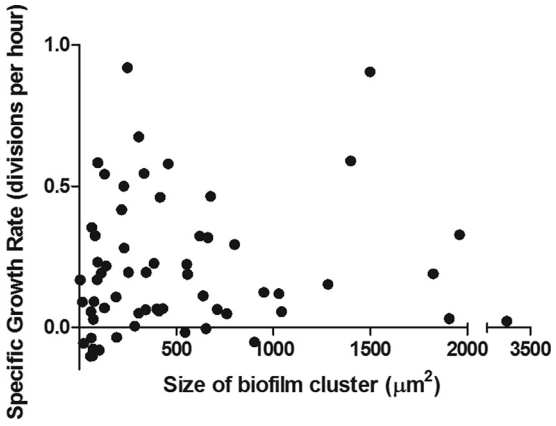

FIG 5 Growth rates versus biofilm aggregate size. Growth rates measured in biofilm clusters in *ex vivo* CF lung tissue are shown as a function of size. There was no significant correlation between size and growth ($P = 0.1891$).

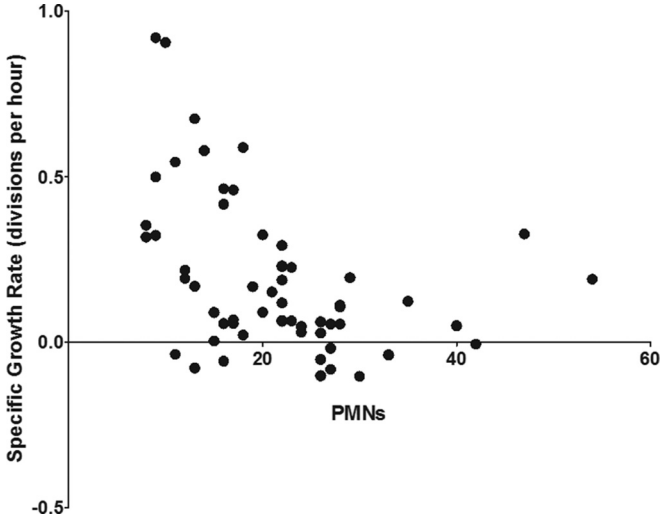

FIG 6 Growth rates measured in lung tissue as a function of the number of surrounding PMNs. The specific *in vivo* growth rate of *Pseudomonas aeruginosa* was estimated by quantitative PNA-FISH as a function of the total number of PMNs within a 20-μm radius from the edge of the 59 measured biofilm aggregates in 20 tissue sections of explanted lungs from three CF patients. There was a significant negative Spearmen's correlation ($\rho = -0.4471$, $P \leq 0.0004$) between the specific growth rate and the number of PMNs in the surrounding mucus.

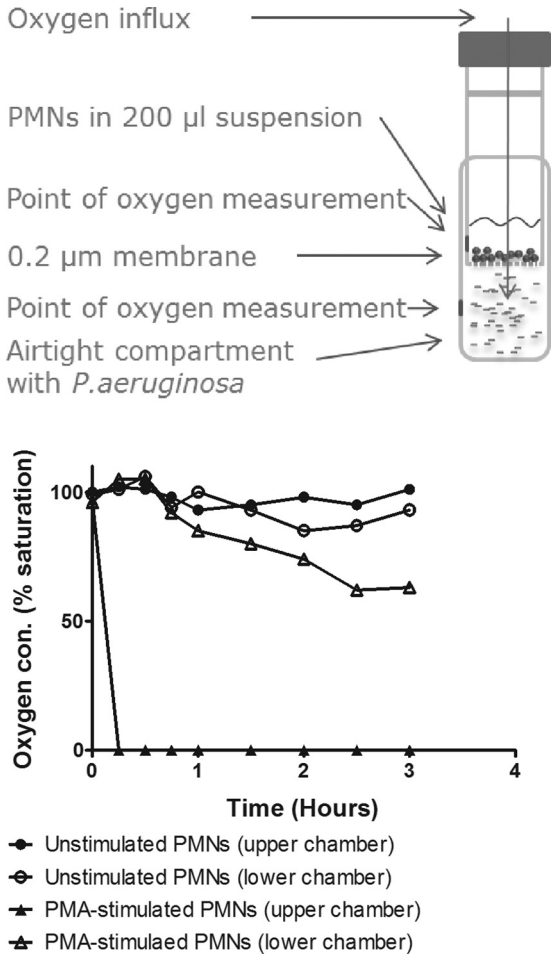

FIG 7 Oxygen consumption by PMNs measured in filter vial. The schematic drawing shows an *in vitro* experiment with PMNs in a chamber separated by a membrane from an airtight chamber containing *P. aeruginosa* (upper panel). O_2 concentration (con) measurements taken in the chamber above the membrane or in the airtight chamber below the membrane were plotted versus time (lower panel). All measurements were done with PMNs (either unstimulated or stimulated with PMA) in the chamber above the membrane.

growth was examined in vials with filters that physically separated PMNs and bacteria within the same chemical environment. Growth rates in the absence or presence of PMNs were determined after 0, 2, and 4 h. O_2 was rapidly depleted in the vials when PMNs were stimulated by PMA (Fig. 7). Quantitative FISH analysis showed significantly lower growth rates of *P. aeruginosa* in the presence of PMNs than in the absence of PMNs after 2 h ($P < 0.0001$) and 4 h ($P < 0.0001$) (Fig. 8A and B). To evaluate whether the PMNs restricted the growth of *P. aeruginosa* by O_2 limitation, the medium was supplemented with an alternative electron acceptor, NO_3^-, which is not affected by PMN metabolism. The growth rate of *P. aeruginosa* in the presence of PMNs and NO_3^- was comparable to that observed without PMNs at both 2 h and 4 h (Fig. 4). The addition of NO_3^- to *P. aeruginosa* in the absence of PMNs did not have any effect on the growth rate.

Growth of *P. aeruginosa* in infected mouse lungs. A pulmonary infection mouse model (21, 28) was used to further elucidate the effect of O_2 partial pressure on the *P. aeruginosa* growth rate. By controlling the size of alginate-embedded *P. aeruginosa* microcolonies, installation of *P. aeruginosa* was predominantly directed to either the conducting zone (large alginate beads) or the respiratory zone (small alginate beads) of mouse lungs. As is known from human physiology, the respiratory zone is oxygenated due to continuous O_2 supply from the venous blood passing alveoli (28). Conversely, the infectious mucus in the bronchi of the conducting zone is anoxic (9). Mice infected with small aggregates showed infection in both the respiratory and conducting airways. In contrast, mice infected with large aggregates showed infection only in the conducting airways. Quantitative PNA-FISH was applied to 34 single aggregates in eight mouse lungs. The *P. aeruginosa* growth rate was significantly higher ($P < 0.008$) in the respiratory airways than in the conducting airways (Fig. 9). To further characterize the effect of aggregate size on the growth rate of immobilized *P. aeruginosa*, the size of each aggregate was measured and correlated to the estimated growth rate. There was no correlation ($P < 0.6$) between the size of the aggregate and the bacterial growth rate.

DISCUSSION

Bacterial biofilm aggregates persist in the conducting zone of the lungs of CF patients despite high-dose antibiotic treatment (4). It has long been speculated that the low growth rates of bacterial cells within chronically infected lungs of CF patients contribute to their tolerance toward antibiotic treatment (29–31), but experimental evidence has been lacking.

In the present study, we demonstrated extremely slow *in vivo* growth of *P. aeruginosa* in the mucus of chronically infected CF lungs. These findings are consistent with the slow growth of *P. aeruginosa* in expectorated CF sputum (18). For the first time, the *in vivo* growth rate of *P. aeruginosa* was directly estimated in a large number of mucus-embedded biofilm aggregates in the lumens of the conducting airways of explanted lungs from three CF patients. These biofilm aggregates had a diameter of 10 to 80 µm and were mostly surrounded by PMNs, in accordance with earlier observations (32). The growth rates among biofilm aggregates in these samples were highly variable, and we could not identify any subpopulations of differentiated growth patterns within the individual biofilm aggregates. Such differential growth patterns of *P. aeruginosa* were previously observed *in vitro* (33–35). Our finding of an undifferentiated growth rate of *P. aeruginosa* aggregates *in vivo* is in accordance with a previous report that calculated a modest (~25%) decrease in the *P. aeruginosa* growth rate for biofilm depths of 40 µm using a continuous-flow biofilm reactor (36). The majority of biofilm aggregates observed in the examined lung samples rarely exceeded 40 µm in diameter. Furthermore, no correlation was found between the size or position of biofilm clusters within the endobronchial mucus in the CF lung tissue and the *P. aeruginosa* growth rate.

The apparent lack of a limiting effect of biofilm aggregate size on *P. aeruginosa* growth *in vivo*, an effect that is typically seen *in vitro*, may be explained by the limited amount of O_2 reaching *P. aeruginosa* biofilm aggregates within mucus plugs, where rapid depletion of O_2 limits aerobic respiration. Worlitzsch et al. (9) demonstrated anoxic conditions in the endobronchial mucus of infected CF patients, and O_2 consumption during the respiratory burst of activated PMNs was proposed as the main cause of the accelerated O_2 depletion in infected mucus (15).

P. aeruginosa growth rates in the biofilm aggregates *in vivo* were compared to the numbers of PMNs surrounding the biofilms. Interestingly, the growth rates in the biofilm aggregates decreased

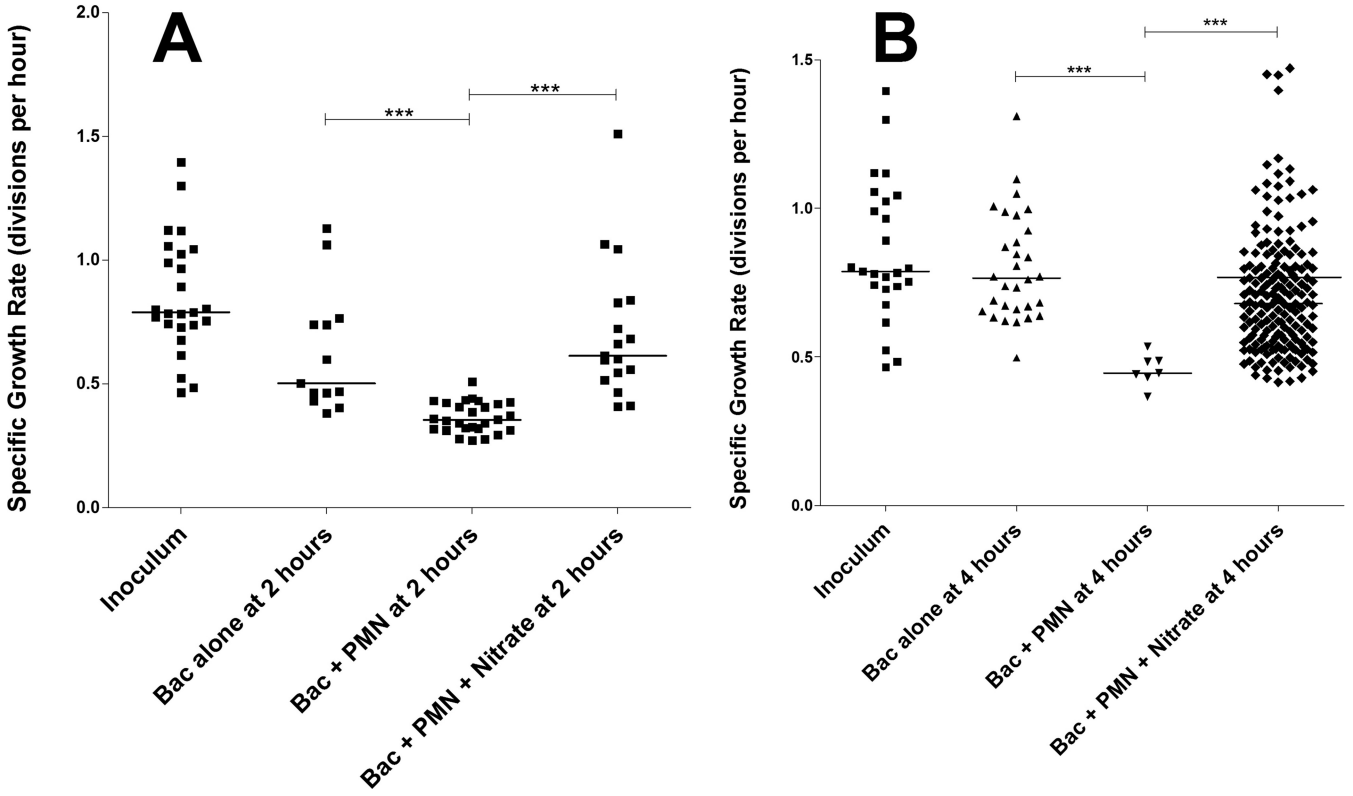

FIG 8 Effects of PMNs on *P. aeruginosa* growth *in vitro*. Changes in the growth rate of *P. aeruginosa* in the absence (Bac alone) or presence (Bac + PMN) of PMNs, untreated or supplemented with NO_3^-, were determined. (A) Growth after 2 h of treatment. (B) Growth after 4 h of treatment. The growth rate was lower in *P. aeruginosa* samples with PMNs than in samples of *P. aeruginosa* alone. The effect of the PMNs could be alleviated by the addition of NO_3^-. The horizontal line represents the median growth rate. ***, $P < 0.001$.

with an increase in the number of PMNs surrounding the biofilm aggregates. The reduction in growth rate may be owing to PMN consumption of O_2, which reduces aerobic respiration in *P. aeruginosa* biofilms (37). Growth rates of *P. aeruginosa* are decreased under low-O_2 conditions (17), possibly because O_2 is an essential electron acceptor for ATP generation during aerobic respiration. By supplying *P. aeruginosa* with NO_3^- as an alternative electron acceptor for anaerobic respiration (38), the limitation of aerobic respiratory metabolism was alleviated, and *P. aeruginosa* growth rates increased significantly, even in the presence of PMNs. We speculate that such conditions are representative of the anoxic environment of *P. aeruginosa* in the endobronchial mucus of CF lungs, where high concentrations of PMNs surround the biofilm aggregates and where the concentration of NO_3^- is sufficiently high to support growth by anaerobic respiration (10, 39).

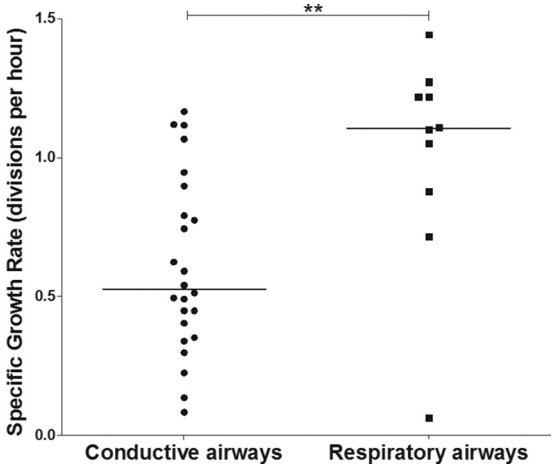

FIG 9 Growth rates of *P. aeruginosa* observed in mouse model. The specific *in vivo* growth rate of *Pseudomonas aeruginosa* was measured in the conducting or respiratory airways of seven mice by quantitative PNA-FISH ($n = 34$ single observations). The growth rate was significantly higher ($P \leq 0.0077$) in respiratory airways than in conducting airways. The horizontal line represents the median growth rate. **, $P \leq 0.01$.

The PMN-induced inhibition of *P. aeruginosa* growth was greatest in biofilms surrounded by approximately 30 PMNs. The growth-inhibitory effect was lower in biofilms surrounded by a higher number of PMNs, perhaps because there is a critical mass of PMNs at which the strong hypoxia approaches complete anoxia. At this point, the absence of O_2 would presumably prevent any further O_2-dependent growth delay by the additional accumulation of PMNs. The slight increase in the *P. aeruginosa* growth rate observed at very high PMN concentrations could be owing to the increased availability of NO_2 and NO_3^-. PMNs can produce both nitrite and nitrate in the CF lung (40), and this may enable the growth of *P. aeruginosa* through anaerobic respiration by denitrification (39). It was also recently shown that PMN production of nitric oxide, which is an intermediate produced during denitrification in infected CF sputum, leads to oxygen consumption (10).

The observed relationship between the *P. aeruginosa* growth rate and the assumed availability of O_2 in CF lungs was confirmed by our findings in a mouse model, where immobilized *P. aeruginosa* grew faster in respiratory airways than in conducting airways. The biofilm aggregates in the alveoli are provided with a continuous supply of O_2 due to their close proximity to the arterial blood supply, in contrast to biofilm aggregates in the conducting airways, where the O_2 availability is lower (28, 41).

Therefore, O_2 availability is a key factor regulating *P. aeruginosa* growth in the lungs of CF patients, and PMNs in infected mucus can inhibit the growth of *P. aeruginosa* by O_2 depletion through their respiratory burst. The aerobic *in vitro* growth of *P. aeruginosa* isolates from CF patients is 2- to 3-fold slower than that of laboratory reference strains, probably owing to genetic adaptation to low-oxygen conditions *in vivo* (19). Besides such adaptations, our data point to an active growth-limiting effect caused by the persisting metabolic state of inflammatory cells that respond to the biofilm aggregates. Therefore, in addition to the decreased lung function associated with endobronchial PMN accumulation (42), bacterial proliferation is also dependent on PMN activity in infected CF lungs.

The increasing growth rate of *P. aeruginosa* in response to NO_3^- supplementation demonstrates that *P. aeruginosa* may be able to continue growing under PMN-induced O_2 depletion by employing anaerobic respiration by denitrification in the infected endobronchial mucus in CF patients. Denitrification by *P. aeruginosa* during chronic lung infection in CF is evidenced by a denitrification biomarker, the porin OprF, in CF sputum (11) and the upregulation of genes for denitrification in CF isolates (13, 14). Furthermore, we recently demonstrated active denitrification in freshly expectorated sputum from CF patients with chronic *P. aeruginosa* infection via measurements of N_2O production (a key intermediate in denitrification) and simultaneous nitrate depletion followed by nitrite depletion (10). Denitrification during chronic lung infection in CF may also be used by other CF pathogens because we recently demonstrated the genetic setup for denitrification as well as anaerobic N_2O production in *Achromobacter xylosoxidans* (43), an emerging CF pathogen that induces an inflammatory response resembling the response induced by *P. aeruginosa* (44). Consumption of glucose by activated PMNs (45, 46) may lead to a reduction in available glucose, which may also limit the growth of *P. aeruginosa* (47, 48). However, the high levels of glucose (2 to 4 mM) in CF airway fluids (49) suggest that bacterial growth in infected mucus is not limited by available glucose. The extent to which the ability of *P. aeruginosa* to grow anaerobically on L-arginine, by substrate-level phosphorylation (50), is affected by the consumption of L-arginine by activated PMNs (51) in CF sputum remains to be firmly established. However, the reportedly high levels (approximately 300 mM) of L-arginine in infected CF sputum (52) do not support growth limitation by L-arginine depletion.

The bactericidal effects of most antibiotics rely on metabolically active, growing bacteria (53). Therefore, our results offer a new possible explanation for why antibiotic treatment can clear bacteria in the respiratory zone but not in the conducting zone of CF lungs (4). Higher *P. aeruginosa* growth rates observed in the respiratory airways of mice with higher O_2 availability may correspond to an infected untreated CF patient. However, when patients are undergoing intravenous administration of antibiotics, the higher growth rate in the respiratory airways, combined with proximity to alveolar capillaries, would result in the improved clearance of *P. aeruginosa* infecting the respiratory zone. In contrast, the low growth rate in the conducting airways protects bacterial cells from antibiotic treatment, and these areas can serve as a reservoir for future recolonization of respiratory airways (2, 4, 18).

In conclusion, our results suggest that PMNs control the growth of *P. aeruginosa* in chronically infected CF lungs. Our demonstration of PMN-related restriction of bacterial growth suggests, for the first time, that a bacteriostatic effect due to intensive O_2 depletion contributes to the antibacterial activity of activated PMNs. However, *P. aeruginosa* seems well adapted to life under constant O_2 depletion by PMNs because the bacteria in the biofilm aggregates can employ anaerobic respiration by denitrification to exploit alternative electron acceptors such as NO_3^-, albeit with a lower energy yield. Such long-term persistence of *P. aeruginosa* under low, but stable, energy conditions may explain its low susceptibility to antibiotic treatment and enable it to adapt to the biofilms of chronically infected CF lungs.

ACKNOWLEDGMENTS

We thank Anne Kirstine Nielsen for excellent technical assistance, Pia Bach Jakobsen for help with DNA/RNA purification, Heidi Marie Paulsen and Lise Strange for cutting CF lung tissue samples, and Bodil Bojsen, Sys Jørgensen, and Anett Wollesen for cutting mouse lung samples. AdvanDx generously supplied the PNA-FISH probes.

Financial support was provided by grants from the Gerda og Aage Haenschs Fond to T.B., the Human Frontier Science Program to T.B., the Lundbeck Foundation to T.B., and the Danish Council for Independent Research to M.K.

We declare that we have no conflicts of interests.

REFERENCES

1. **Koch C, Hoiby N.** 2000. Diagnosis and treatment of cystic fibrosis. Respiration **67:**239–247. http://dx.doi.org/10.1159/000029503.
2. **Hoiby N.** 2011. Recent advances in the treatment of *Pseudomonas aeruginosa* infections in cystic fibrosis. BMC Med. **9:**32. http://dx.doi.org/10.1186/1741-7015-9-32.
3. **Alhede M, Bjarnsholt T, Jensen PO, Phipps RK, Moser C, Christophersen L, Christensen LD, van Gennip M, Parsek M, Hoiby N, Rasmussen TB, Givskov M.** 2009. *Pseudomonas aeruginosa* recognizes and responds aggressively to the presence of polymorphonuclear leukocytes. Microbiology **155:**3500–3508. http://dx.doi.org/10.1099/mic.0.031443-0.
4. **Bjarnsholt T, Jensen PO, Fiandaca MJ, Pedersen J, Hansen CR, Andersen CB, Pressler T, Givskov M, Hoiby N.** 2009. *Pseudomonas aeruginosa* biofilms in the respiratory tract of cystic fibrosis patients. Pediatr. Pulmonol. **44:**547–558. http://dx.doi.org/10.1002/ppul.21011.
5. **Høiby N, Ciofu O, Johansen HK, Song ZJ, Moser C, Jensen PO, Molin S, Givskov M, Tolker-Nielsen T, Bjarnsholt T.** 2011. The clinical impact of bacterial biofilms. Int. J. Oral Sci. **3:**55–65. http://dx.doi.org/10.4248/IJOS11026.
6. **O'Toole GA.** 2003. To build a biofilm. J. Bacteriol. **185:**2687–2689. http://dx.doi.org/10.1128/JB.185.9.2687-2689.2003.
7. **Evans DJ, Allison DG, Brown MR, Gilbert P.** 1991. Susceptibility of *Pseudomonas aeruginosa* and *Escherichia coli* biofilms towards ciprofloxacin: effect of specific growth rate. J. Antimicrob. Chemother. **27:**177–184. http://dx.doi.org/10.1093/jac/27.2.177.
8. **Borriello G, Werner E, Roe F, Kim AM, Ehrlich GD, Stewart PS.** 2004. Oxygen limitation contributes to antibiotic tolerance of *Pseudomonas aeruginosa* in biofilms. Antimicrob. Agents Chemother. **48:**2659–2664. http://dx.doi.org/10.1128/AAC.48.7.2659-2664.2004.
9. **Worlitzsch D, Tarran R, Ulrich M, Schwab U, Cekici A, Meyer KC, Birrer P, Bellon G, Berger J, Weiss T, Botzenhart K, Yankaskas JR, Randell S, Boucher RC, Doring G.** 2002. Effects of reduced mucus oxygen concentration in airway *Pseudomonas* infections of cystic fibrosis patients. J. Clin. Invest. **109:**317–325. http://dx.doi.org/10.1172/JCI13870.
10. **Kolpen M, Kuhl M, Bjarnsholt T, Moser C, Hansen CR, Liengaard L,**

Kharazmi A, Pressler T, Hoiby N, Jensen PO. 2014. Nitrous oxide production in sputum from cystic fibrosis patients with chronic *Pseudomonas aeruginosa* lung infection. PLoS One **9:**e84353. http://dx.doi.org/10.1371/journal.pone.0084353.

11. **Yoon SS, Hennigan RF, Hilliard GM, Ochsner UA, Parvatiyar K, Kamani MC, Allen HL, DeKievit TR, Gardner PR, Schwab U, Rowe JJ, Iglewski BH, McDermott TR, Mason RP, Wozniak DJ, Hancock RE, Parsek MR, Noah TL, Boucher RC, Hassett DJ.** 2002. *Pseudomonas aeruginosa* anaerobic respiration in biofilms: relationships to cystic fibrosis pathogenesis. Dev. Cell **3:**593–603. http://dx.doi.org/10.1016/S1534-5807(02)00295-2.
12. **Beckmann C, Brittnacher M, Ernst R, Mayer-Hamblett N, Miller SI, Burns JL.** 2005. Use of phage display to identify potential *Pseudomonas aeruginosa* gene products relevant to early cystic fibrosis airway infections. Infect. Immun. **73:**444–452. http://dx.doi.org/10.1128/IAI.73.1.444-452.2005.
13. **Son MS, Matthews WJ, Jr, Kang Y, Nguyen DT, Hoang TT.** 2007. *In vivo* evidence of *Pseudomonas aeruginosa* nutrient acquisition and pathogenesis in the lungs of cystic fibrosis patients. Infect. Immun. **75:**5313–5324. http://dx.doi.org/10.1128/IAI.01807-06.
14. **Lee B, Schjerling CK, Kirkby N, Hoffmann N, Borup R, Molin S, Hoiby N, Ciofu O.** 2011. Mucoid *Pseudomonas aeruginosa* isolates maintain the biofilm formation capacity and the gene expression profiles during the chronic lung infection of CF patients. APMIS **119:**263–274. http://dx.doi.org/10.1111/j.1600-0463.2011.02726.x.
15. **Kolpen M, Hansen CR, Bjarnsholt T, Moser C, Christensen LD, van Gennip M, Ciofu O, Mandsberg L, Kharazmi A, Doring G, Givskov M, Hoiby N, Jensen PO.** 2010. Polymorphonuclear leucocytes consume oxygen in sputum from chronic *Pseudomonas aeruginosa* pneumonia in cystic fibrosis. Thorax **65:**57–62. http://dx.doi.org/10.1136/thx.2009.114512.
16. **Babior BM, Curnutte JT, McMurrich BJ.** 1976. The particulate superoxide-forming system from human neutrophils. Properties of the system and further evidence supporting its participation in the respiratory burst. J. Clin. Invest. **58:**989–996.
17. **Alvarez-Ortega C, Harwood CS.** 2007. Responses of *Pseudomonas aeruginosa* to low oxygen indicate that growth in the cystic fibrosis lung is by aerobic respiration. Mol. Microbiol. **65:**153–165. http://dx.doi.org/10.1111/j.1365-2958.2007.05772.x.
18. **Yang L, Haagensen JA, Jelsbak L, Johansen HK, Sternberg C, Hoiby N, Molin S.** 2008. In situ growth rates and biofilm development of *Pseudomonas aeruginosa* populations in chronic lung infections. J. Bacteriol. **190:**2767–2776. http://dx.doi.org/10.1128/JB.01581-07.
19. **Rau MH, Hansen SK, Johansen HK, Thomsen LE, Workman CT, Nielsen KF, Jelsbak L, Hoiby N, Yang L, Molin S.** 2010. Early adaptive developments of *Pseudomonas aeruginosa* after the transition from life in the environment to persistent colonization in the airways of human cystic fibrosis hosts. Environ. Microbiol. **12:**1643–1658. http://dx.doi.org/10.1111/j.1462-2920.2010.02211.x.
20. **Bachmann B.** 1996. Derivations and genotypes of some mutant derivatives of *Escherichia coli* K-12, p 2460–2488. *In* Neidhardt FC, Curtiss R, III, Ingraham JL, Lin ECC, Low KB, Magasanik B, Reznikoff WS, Riley M, Schaechter M, Umbarger HE (ed), *Escherichia coli* and *Salmonella*: cellular and molecular biology, 2nd ed. ASM Press, Washington, DC.
21. **Christophersen LJ, Trostrup H, Malling Damlund DS, Bjarnsholt T, Thomsen K, Jensen PO, Hougen HP, Hoiby N, Moser C.** 2012. Bead-size directed distribution of *Pseudomonas aeruginosa* results in distinct inflammatory response in a mouse model of chronic lung infection. Clin. Exp. Immunol. **170:**222–230. http://dx.doi.org/10.1111/j.1365-2249.2012.04652.x.
22. **Perry-O'Keefe H, Rigby S, Oliveira K, Sorensen D, Stender H, Coull J, Hyldig-Nielsen JJ.** 2001. Identification of indicator microorganisms using a standardized PNA FISH method. J. Microbiol. Methods **47:**281–292. http://dx.doi.org/10.1016/S0167-7012(01)00303-7.
23. **Bjarnsholt T, Jensen PO, Burmolle M, Hentzer M, Haagensen JA, Hougen HP, Calum H, Madsen KG, Moser C, Molin S, Hoiby N, Givskov M.** 2005. *Pseudomonas aeruginosa* tolerance to tobramycin, hydrogen peroxide and polymorphonuclear leukocytes is quorum-sensing dependent. Microbiology **151:**373–383. http://dx.doi.org/10.1099/mic.0.27463-0.
24. **Kuhl M.** 2005. Optical microsensors for analysis of microbial communities. Methods Enzymol. **397:**166–199. http://dx.doi.org/10.1016/S0076-6879(05)97010-9.
25. **Rickelt LF, Askaer L, Walpersdorf E, Elberling B, Glud RN, Kühl M.** 2013. An optode sensor array for long term in situ measurements of O2 in soil and sediment. J. Environ. Qual. **42:**1267–1273. http://dx.doi.org/10.2134/jeq2012.0334.
26. **Schaechter M, Maaloe O, Kjeldgaard NO.** 1958. Dependency on medium and temperature of cell size and chemical composition during balanced grown of *Salmonella* typhimurium. J. Gen. Microbiol. **19:**592–606. http://dx.doi.org/10.1099/00221287-19-3-592.
27. **Baldridge CW, Gerard RW.** 1932. The extra respiration of phagocytosis. Am. J. Physiol. **103:**235–236.
28. **West.** 2000. Respiratory physiology: the essentials, 6th ed. Lippincott, Williams, and Wilkins, Baltimore, MD.
29. **Keren I, Kaldalu N, Spoering A, Wang Y, Lewis K.** 2004. Persister cells and tolerance to antimicrobials. FEMS Microbiol. Lett. **230:**13–18. http://dx.doi.org/10.1016/S0378-1097(03)00856-5.
30. **Costerton JW, Lewandowski Z, Caldwell DE, Korber DR, Lappin-Scott HM.** 1995. Microbial biofilms. Annu. Rev. Microbiol. **49:**711–745. http://dx.doi.org/10.1146/annurev.mi.49.100195.003431.
31. **Hoiby N, Bjarnsholt T, Givskov M, Molin S, Ciofu O.** 2010. Antibiotic resistance of bacterial biofilms. Int. J. Antimicrob. Agents **35:**322–332. http://dx.doi.org/10.1016/j.ijantimicag.2009.12.011.
32. **Bjarnsholt T, Alhede M, Eickhardt-Sorensen SR, Moser C, Kuhl M, Jensen PO, Hoiby N.** 2013. The in vivo biofilm. Trends Microbiol. **21:**466–474. http://dx.doi.org/10.1016/j.tim.2013.06.002.
33. **Wentland EJ, Stewart PS, Huang CT, McFeters GA.** 1996. Spatial variations in growth rate within *Klebsiella pneumoniae* colonies and biofilm. Biotechnol. Prog. **12:**316–321. http://dx.doi.org/10.1021/bp9600243.
34. **Williamson KS, Richards LA, Perez-Osorio AC, Pitts B, McInnerney K, Stewart PS, Franklin MJ.** 2012. Heterogeneity in *Pseudomonas aeruginosa* biofilms includes expression of ribosome hibernation factors in the antibiotic-tolerant subpopulation and hypoxia-induced stress response in the metabolically active population. J. Bacteriol. **194:**2062–2073. http://dx.doi.org/10.1128/JB.00022-12.
35. **Stewart PS, Franklin MJ.** 2008. Physiological heterogeneity in biofilms. Nat. Rev. Microbiol. **6:**199–210. http://dx.doi.org/10.1038/nrmicro1838.
36. **Roberts ME, Stewart PS.** 2005. Modelling protection from antimicrobial agents in biofilms through the formation of persister cells. Microbiology **151:**75–80. http://dx.doi.org/10.1099/mic.0.27385-0.
37. **Jesaitis AJ, Franklin MJ, Berglund D, Sasaki M, Lord CI, Bleazard JB, Duffy JE, Beyenal H, Lewandowski Z.** 2003. Compromised host defense on *Pseudomonas aeruginosa* biofilms: characterization of neutrophil and biofilm interactions. J. Immunol. **171:**4329–4339. http://dx.doi.org/10.4049/jimmunol.171.8.4329.
38. **Zumft WG.** 1997. Cell biology and molecular basis of denitrification. Microbiol. Mol. Biol. Rev. **61:**533–616.
39. **Palmer KL, Brown SA, Whiteley M.** 2007. Membrane-bound nitrate reductase is required for anaerobic growth in cystic fibrosis sputum. J. Bacteriol. **189:**4449–4455. http://dx.doi.org/10.1128/JB.00162-07.
40. **Francoeur C, Denis M.** 1995. Nitric oxide and interleukin-8 as inflammatory components of cystic fibrosis. Inflammation **19:**587–598. http://dx.doi.org/10.1007/BF01539138.
41. **Hogg JC.** 2004. Pathophysiology of airflow limitation in chronic obstructive pulmonary disease. Lancet **364:**709–721. http://dx.doi.org/10.1016/S0140-6736(04)16900-6.
42. **Mayer-Hamblett N, Aitken ML, Accurso FJ, Kronmal RA, Konstan MW, Burns JL, Sagel SD, Ramsey BW.** 2007. Association between pulmonary function and sputum biomarkers in cystic fibrosis. Am. J. Respir. Crit. Care Med. **175:**822–828. http://dx.doi.org/10.1164/rccm.200609-1354OC.
43. **Jakobsen TH, Hansen MA, Jensen PO, Hansen L, Riber L, Cockburn A, Kolpen M, Ronne Hansen C, Ridderberg W, Eickhardt S, Hansen M, Kerpedjiev P, Alhede M, Qvortrup K, Burmolle M, Moser C, Kuhl M, Ciofu O, Givskov M, Sorensen SJ, Hoiby N, Bjarnsholt T.** 2013. Complete genome sequence of the cystic fibrosis pathogen *Achromobacter xylosoxidans* NH44784 to 1996 complies with important pathogenic phenotypes. PLoS One **8:**e68484. http://dx.doi.org/10.1371/journal.pone.0068484.
44. **Hansen CR, Pressler T, Nielsen KG, Jensen PO, Bjarnsholt T, Hoiby N.** 2010. Inflammation in *Achromobacter xylosoxidans* infected cystic fibrosis patients. J. Cyst. Fibros. **9:**51–58. http://dx.doi.org/10.1016/j.jcf.2009.10.005.
45. **Borregaard N, Herlin T.** 1982. Energy metabolism of human neutrophils during phagocytosis. J. Clin. Invest. **70:**550–557. http://dx.doi.org/10.1172/JCI110647.

46. **Laval J, Touhami J, Herzenberg LA, Conrad C, Taylor N, Battini JL, Sitbon M, Tirouvanziam R.** 2013. Metabolic adaptation of neutrophils in cystic fibrosis airways involves distinct shifts in nutrient transporter expression. J. Immunol. **190:**6043–6050. http://dx.doi.org/10.4049/jimmunol.1201755.
47. **Palmer KL, Aye LM, Whiteley M.** 2007. Nutritional cues control *Pseudomonas aeruginosa* multicellular behavior in cystic fibrosis sputum. J. Bacteriol. **189:**8079–8087. http://dx.doi.org/10.1128/JB.01138-07.
48. **Brennan AL, Gyi KM, Wood DM, Johnson J, Holliman R, Baines DL, Philips BJ, Geddes DM, Hodson ME, Baker EH.** 2007. Airway glucose concentrations and effect on growth of respiratory pathogens in cystic fibrosis. J. Cyst. Fibros. **6:**101–109. http://dx.doi.org/10.1016/j.jcf.2006.03.009.
49. **Baker EH, Clark N, Brennan AL, Fisher DA, Gyi KM, Hodson ME, Philips BJ, Baines DL, Wood DM.** 2007. Hyperglycemia and cystic fibrosis alter respiratory fluid glucose concentrations estimated by breath condensate analysis. J. Appl. Physiol. **102:**1969–1975. http://dx.doi.org/10.1152/japplphysiol.01425.2006.
50. **Vander Wauven C, Pierard A, Kley-Raymann M, Haas D.** 1984. *Pseudomonas aeruginosa* mutants affected in anaerobic growth on arginine: evidence for a four-gene cluster encoding the arginine deiminase pathway. J. Bacteriol. **160:**928–934.
51. **Chen LY, Mehta JL.** 1996. Variable effects of L-arginine analogs on L-arginine-nitric oxide pathway in human neutrophils and platelets may relate to different nitric oxide synthase isoforms. J. Pharmacol. Exp. Ther. **276:**253–257.
52. **Grasemann H, Tullis E, Ratjen F.** 2013. A randomized controlled trial of inhaled L-arginine in patients with cystic fibrosis. J. Cyst. Fibros. **12:**468–474. http://dx.doi.org/10.1016/j.jcf.2012.12.008.
53. **Eng RH, Padberg FT, Smith SM, Tan EN, Cherubin CE.** 1991. Bactericidal effects of antibiotics on slowly growing and nongrowing bacteria. Antimicrob. Agents Chemother. **35:**1824–1828. http://dx.doi.org/10.1128/AAC.35.9.1824.
54. **Carreras MC, Pargament GA, Catz SD, Poderoso JJ, Boveris A.** 1994. Kinetics of nitric oxide and hydrogen peroxide production and formation of peroxynitrite during the respiratory burst of human neutrophils. FEBS Lett. **341:**65–68. http://dx.doi.org/10.1016/0014-5793(94)80241-6.
55. **Alderton WK, Cooper CE, Knowles RG.** 2001. Nitric oxide synthases: structure, function and inhibition. Biochem. J. **357**(Pt 3):593–615.